

Dynamics of the Madden Julian Oscillation (DYNAMO) 2011 NOAA P-3 Tail X-band Doppler Radar Data Summary

PI: David P. Jorgensen
120 David L. Boren Blvd.
Norman, OK 73072

Authors:

Nick Guy (Nick.Guy@noaa.gov)

David Jorgensen (David.P.Jorgensen@noaa.gov)

Updated 14 November 2013

1. Dataset Overview

The NOAA P-3 aircraft flew missions from 11 November – 13 December 2011. The tail-mounted radar provided detailed 3D information of convective cloud reflectivity and Doppler velocity with focus on storm structure variability and (up- and down-) scale interactions of mesoscale convective systems during distinct MJO phases. Multiple “modules” were designed to acquire data for specific scientific purposes. This dataset consists of the radar convective element (RCE) module (Fig. 1) flight patterns. An overview of the modules can be found in Table 1.

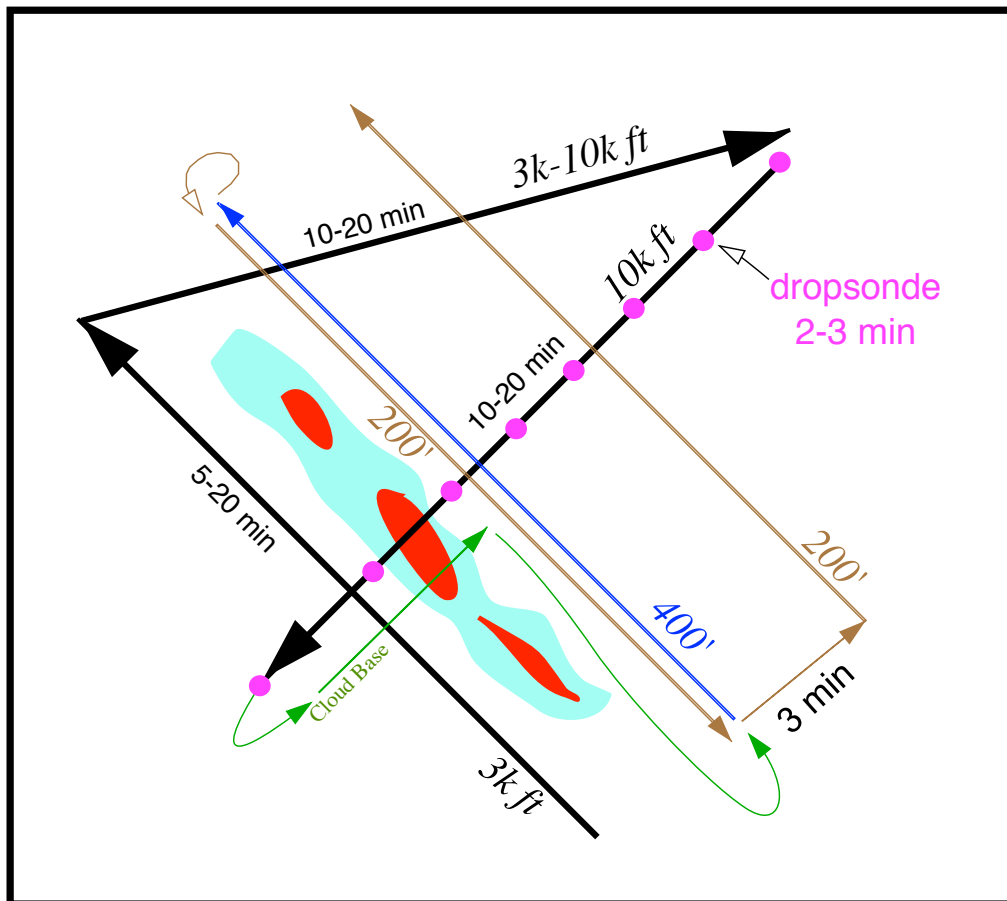


Figure 1. Radar convective element (RCE) module flight pattern. Designed to sample both the convective and stratiform portions, providing 3-dimensional reflectivity and kinematic information.

Table 1. Outline of the 10 RCE modules obtained during the DYNAMO campaign.

Date (2011)	Duration (UTC)	Meteorological Category
11 November	0902-0923	Suppressed, Isolated convection

16 November	0421-0519	Scattered, ITCZ
22 November	0433-0515	Active, MCS
	0635-0731	
24 November	0351-0457	MJO, MCS
	0705-0745	
30 November	0809-0854	MJO, Scattered convection
8 December	0610-0640	Suppressed, Isolated convection
	0642-0717	

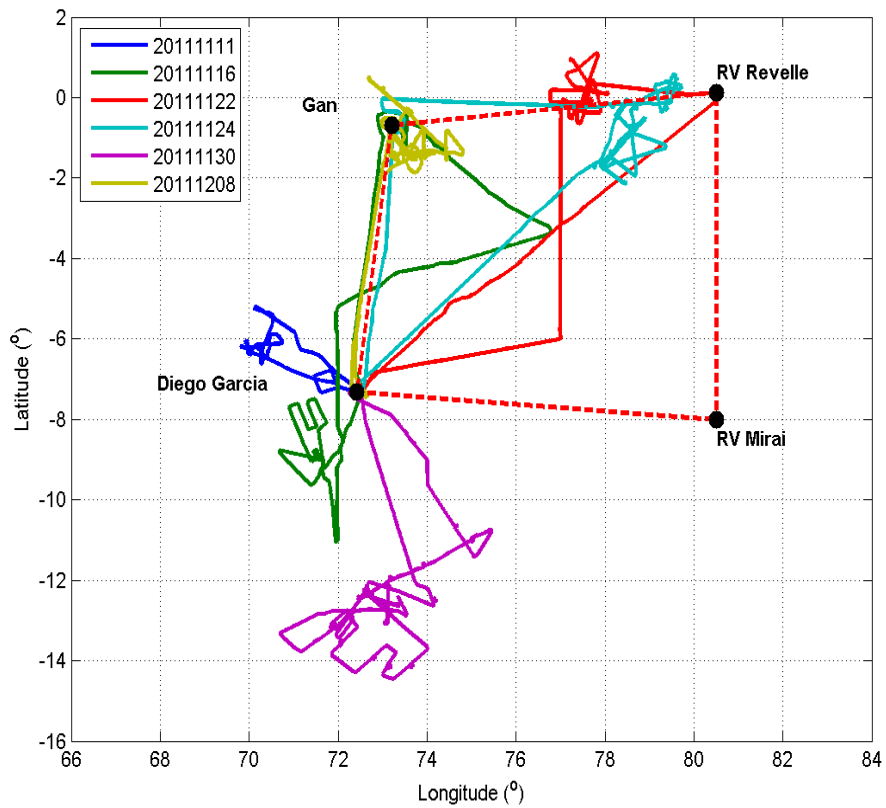


Figure 2. Locations of each RCE module. See Table 1 for temporal extent and meteorological characteristics

2. Instrument Description

The tail-mounted radar is a vertically-scanning (about the aircraft longitudinal axis) X-band radar system (Jorgensen et al. 1983). The fore-aft scanning technique (FAST; Jorgensen et al. 1996) is employed where the antenna alternates between a scan at a 20° forward-pointing angle followed by a 20° backward-pointing angle (from the plane normal to the flight track). Radar characteristics can be found in Table 2.

Each 360° rotation is recorded as a sweep. The scan rate results in a pair of fore and aft sweeps recorded approximately every 12 seconds. With typical P-3 aircraft ground speeds ($\sim 120 \text{ m s}^{-1}$), horizontal spacing is approximately 1.4 km. The FAST technique results in a criss-crossing grid guaranteeing two independent measurements at each point where the radar beams overlap. The use of batched, dual pulse repetition frequencies (PRFs) allows the Nyquist velocity to be extended well beyond that constrained by radar characteristics (Jorgensen et al. 2000).

Table 2 Characteristics of the tail-mounted P-3 X-band radar.

wavelength	3.22 cm (X-band)
PRF	3200/2400 s^{-1}
R_{max}	38 km
V_{max}	$\pm 51 \text{ m s}^{-1}$
H beamwidth	1.35°
V beamwidth	1.90°
Pulse width	0.25/0.375 μs
Gate length	150 m
Antenna rotation	10 rpm (60° s^{-1})

3. Data Processing

3.1. Quality Control

The quality control procedure is a two-phase process, both performed in the Soloii software package maintained by the National Center for Atmospheric Research (NCAR). First the data is run through a series of automated algorithms and second hand-editing is performed to remove any remaining non-meteorological information. A flow chart of the process can be found in Figure 3 and a more detailed process follows.

Surface return is removed through a geometrical calculation using aircraft altitude and surface topography information (null in this experiment due to collection of data over the ocean surface).

Data is run through a filter that inserts bad data flags for all points exhibiting large values of spectrum width, which helps remove 2nd trip echo and other suspect data. This threshold value was tuned to this particular dataset for optimum performance

The next filter was designed to (at least partially) remove the reflectivity “ring” caused by side lobe return from the sea surface. A minimum reflectivity and maximum spectrum width were used to screen out the majority of false echo caused by this phenomenon. Again, the thresholds were tuned for this dataset.

Defreckling and despeckling routines in Soloii were used to clean up the data in areas of non-homogeneous and non-meteorological echo.

Each individual sweep was analyzed and any remaining non-meteorological echo was removed by hand.

An example of the raw and quality controlled reflectivity field is shown in Figure 4.

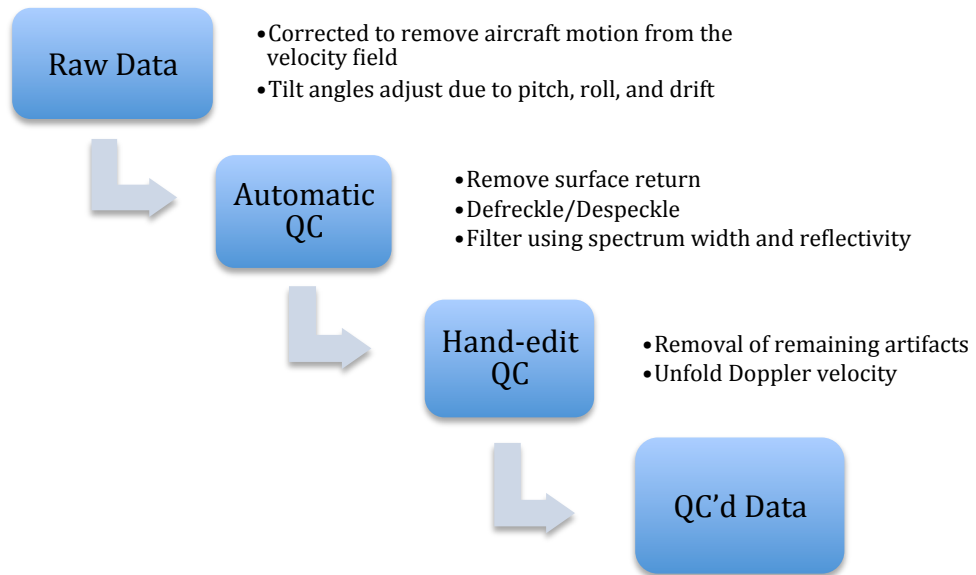


Figure 3 Flow chart of quality control procedures applied to the radar data for the DYNAMO project.

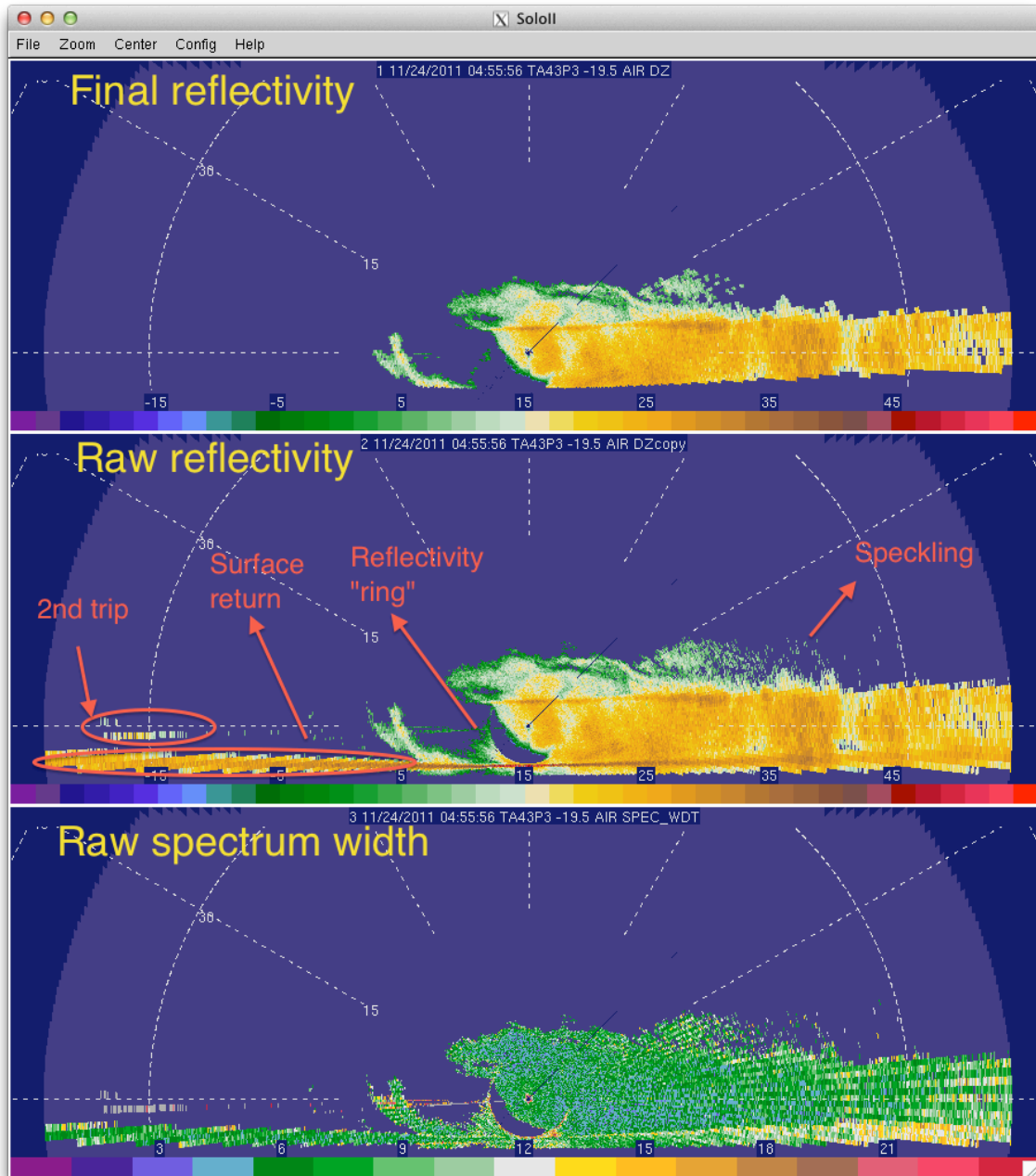


Figure 4 An example showing before and after quality control procedure was performed to remove non-meteorological radar echo.

3.2. Wind Synthesis

A pseudo-dual-Doppler approach (Jorgensen et al. 1996) was employed on the edited data to construct 3-D wind fields. Terminal fall speeds of precipitation were removed from radial velocity estimates using empirical equations relating radar reflectivity and terminal fall speed. Different relationships were used for rain below 4 km (Joss and Waldvogel 1970) and snow above 4.5 km (Atlas et al. 1973). Between 4 and 4.5 km, a weighted average of the rain and snow relationships was computed. These

heights agree well with climatological tropical freezing level heights, and with dropsonde measurements. The maximum reflectivity associated with each grid point in cases where more than one beam intersected a co-located point was used, along with the accompanying Doppler velocity.

Horizontal winds (u, v) were computed from radial velocities using an over-determined, two-equation solution. The two-equation system is a function of the zonal (u), meridional (v), and vertical (w) wind components. A two-pass Leise filter (Leise 1981) was applied to horizontal winds to reduce noise resulting from features 3-4 times the horizontal grid spacing (6 – 7.5 km). Once solutions for u and v were found, vertical velocity was estimated through upward integration of the continuity equation, with a boundary condition of $w = 0$ assumed at the surface. Vertical column mass balance was achieved by applying the (O'Brien 1970) correction to the divergence profile through setting $w = 0$ at echo top.

4. Data Format

4.1. Radar Coordinate Data

Radar data are stored in polar coordinate DORADE format. Information regarding the DORADE format can be found at http://www.ral.ucar.edu/projects/titan/docs/radial_formats/. All fore-aft sweep pairs has been collected into one “volume” file for each RCE listed in Table 1, resulting in a total of 10 files. Variables include quality-controlled fields of radar reflectivity (DZ) and Doppler velocity (VG), along with variables containing the raw data for radar reflectivity (DZcopy), Doppler velocity (VGcopy), and spectrum width (SPEC_WDT). It should be noted that corrections for aircraft motion have been removed from the velocity field. An additional field for Doppler velocity with no correction for aircraft motion (VE) is also included. Corrections accounting for aircraft pitch, roll, and drift have been applied to the tilt angles for all data.

The naming convention of the files is “YYYYMMDD.HHmm.N43P3.dor” where YYYY=year, MM=month, DD=day, HH=hour, and mm=min, where times are in UTC and indicate the beginning of the flight module. The N43P3 is the aircraft identifier.

Missing data is flagged by a value of -999.

This dataset is the processed data as of 1 October 2012, and is the final dataset. Other modules mentioned previously can be processed upon request.

4.2. Gridded Analysis Data

The wind synthesis data are stored in classic NetCDF format, created using the NCAR Command Language (NCL). Variables include quality-controlled fields of radar reflectivity (dBZ) and east-west (U) and north-south (V) relative winds, vertical wind speeds (W), divergence (Div) along with

variables containing supplementary information on the data properties. In addition global attributes have been included for a quick-look at processing details for those familiar with this analysis. For further details, please contact the authors of this documentation.

The naming convention of the files is “YYYYMMDD_HHmm_N43P3_windsyn.nc” where YYYY=year, MM=month, DD=day, HH=hour, and mm=min, where times are in UTC and indicate the beginning of the flight module. The N43P3 is the aircraft identifier. Missing data is flagged by a value of -999.

This dataset is the processed data as of 14 November 2013, and is the final dataset. Other modules mentioned previously can be processed upon request.

5. Data Remarks

5.1. Radar Coordinate Data

16 November case exhibited substantial “smearing” of rays
28 November case showed small amount of “smearing” especially during the 0400 hour
Some small gaps in data collection from data processor “freezing up”
Some modules have sector scans in which only one side of aircraft was scanned after a turn when convection was present on both sides

6. References

- Atlas, D., R. C. Srivastava, and R. S. Sekhon, 1973: Doppler radar characteristics of precipitation at vertical incidence. *Rev. Geophys.*, **11**, 1–35, doi:10.1029/RG011i001p00001.
- Jorgensen, D. P., P. H. Hildebrand, and C. L. Frush, 1983: Feasibility test of an airborne pulse-Doppler meteorological radar. *J. Climate Appl. Meteor.*, **22**, 744–757, doi:10.1175/1520-0450(1983)022<0744:FTO AAP>2.0.CO;2.
- Jorgensen, D. P., T. Matejka, and J. D. DuGranrut, 1996: Multi-beam techniques for deriving wind fields from airborne Doppler radars. *Meteor. Atmos. Phys.*, **59**, 83–104, doi:10.1007/BF01032002.
- Jorgensen, D. P., T. R. Shepherd, and A. S. Goldstein, 2000: A dual-pulse repetition frequency scheme for mitigating velocity ambiguities of the NOAA P-3 airborne Doppler radar. *J. Atmos. Oceanic Technol.*, **17**, 585–594, doi:10.1175/1520-0426(2000)017<0585:ADPRFS>2.0.CO;2.
- Joss, J., and A. Waldvogel, 1970: Raindrop size distribution and Doppler velocities. *Preprints*, 14th Conf. on Radar Meteorology, Tucson, AZ, Amer. Meteor. Soc., 153–156.

Leise, J. A., 1981: *A multidimensional scale-telescoped filter and data extension package.*

O'Brien, J. J., 1970: Alternative Solutions to the Classical Vertical Velocity Problem. *J. Appl. Meteor.*, **9**, 197–203, doi:10.1175/1520-0450(1970)009<0197:ASTTCV>2.0.CO;2.